

Search for anomalous Wtb couplings in single top quark production in $p\bar{p}$ collisions at $\sqrt{s} = 1.96$ TeV

V.M. Abazov,³⁴ B. Abbott,⁷² B.S. Acharya,²⁸ M. Adams,⁴⁸ T. Adams,⁴⁶ G.D. Alexeev,³⁴ G. Alkhalaf,³⁸ A. Alton^a,⁶⁰ G. Alverson,⁵⁹ G.A. Alves,² M. Aoki,⁴⁷ A. Askew,⁴⁶ B. Åsman,⁴⁰ S. Atkins,⁵⁷ O. Atramentov,⁶⁴ K. Augsten,⁹ C. Avila,⁷ J. BackusMayes,⁷⁹ F. Badaud,¹² L. Bagby,⁴⁷ B. Baldin,⁴⁷ D.V. Bandurin,⁴⁶ S. Banerjee,²⁸ E. Barberis,⁵⁹ P. Baringer,⁵⁵ J. Barreto,³ J.F. Bartlett,⁴⁷ U. Bassler,¹⁷ V. Bazterra,⁴⁸ A. Bean,⁵⁵ M. Begalli,³ C. Belanger-Champagne,⁴⁰ L. Bellantoni,⁴⁷ S.B. Beri,²⁶ G. Bernardi,¹⁶ R. Bernhard,²¹ I. Bertram,⁴¹ M. Besançon,¹⁷ R. Beuselinck,⁴² V.A. Bezzubov,³⁷ P.C. Bhat,⁴⁷ V. Bhatnagar,²⁶ G. Blazey,⁴⁹ S. Blessing,⁴⁶ K. Bloom,⁶³ A. Boehnlein,⁴⁷ D. Boline,⁶⁹ E.E. Boos,³⁶ G. Borissov,⁴¹ T. Bose,⁵⁸ A. Brandt,⁷⁵ O. Brandt,²² R. Brock,⁶¹ G. Brooijmans,⁶⁷ A. Bross,⁴⁷ D. Brown,¹⁶ J. Brown,¹⁶ X.B. Bu,⁴⁷ M. Buehler,⁴⁷ V. Buescher,²³ V. Bunichev,³⁶ S. Burdin,^b,⁴¹ T.H. Burnett,⁷⁹ C.P. Buszello,⁴⁰ B. Calpas,¹⁴ E. Camacho-Pérez,³¹ M.A. Carrasco-Lizarraga,⁵⁵ B.C.K. Casey,⁴⁷ H. Castilla-Valdez,³¹ S. Chakrabarti,⁶⁹ D. Chakraborty,⁴⁹ K.M. Chan,⁵³ A. Chandra,⁷⁷ E. Chapon,¹⁷ G. Chen,⁵⁵ S. Chevalier-Théry,¹⁷ D.K. Cho,⁷⁴ S.W. Cho,³⁰ S. Choi,³⁰ B. Choudhary,²⁷ S. Cihangir,⁴⁷ D. Claes,⁶³ J. Clutter,⁵⁵ M. Cooke,⁴⁷ W.E. Cooper,⁴⁷ M. Corcoran,⁷⁷ F. Couderc,¹⁷ M.-C. Cousinou,¹⁴ A. Croc,¹⁷ D. Cutts,⁷⁴ A. Das,⁴⁴ G. Davies,⁴² K. De,⁷⁵ S.J. de Jong,³³ E. De La Cruz-Burelo,³¹ F. Déliot,¹⁷ R. Demina,⁶⁸ D. Denisov,⁴⁷ S.P. Denisov,³⁷ S. Desai,⁴⁷ C. Deterre,¹⁷ K. DeVaughan,⁶³ H.T. Diehl,⁴⁷ M. Diesburg,⁴⁷ P.F. Ding,⁴³ A. Dominguez,⁶³ T. Dorland,⁷⁹ A. Dubey,²⁷ L.V. Dudko,³⁶ D. Duggan,⁶⁴ A. Duperrin,¹⁴ S. Dutt,²⁶ A. Dyshkant,⁴⁹ M. Eads,⁶³ D. Edmunds,⁶¹ J. Ellison,⁴⁵ V.D. Elvira,⁴⁷ Y. Enari,¹⁶ H. Evans,⁵¹ A. Evdokimov,⁷⁰ V.N. Evdokimov,³⁷ G. Facini,⁵⁹ T. Ferbel,⁶⁸ F. Fiedler,²³ F. Filthaut,³³ W. Fisher,⁶¹ H.E. Fisk,⁴⁷ M. Fortner,⁴⁹ H. Fox,⁴¹ S. Fuess,⁴⁷ A. Garcia-Bellido,⁶⁸ G.A. García-Guerra^c,³¹ V. Gavrilov,³⁵ P. Gay,¹² W. Geng,^{14,61} D. Gerbaudo,⁶⁵ C.E. Gerber,⁴⁸ Y. Gershtein,⁶⁴ G. Ginther,^{47,68} G. Golovanov,³⁴ A. Goussiou,⁷⁹ P.D. Grannis,⁶⁹ S. Greder,¹⁸ H. Greenlee,⁴⁷ Z.D. Greenwood,⁵⁷ E.M. Gregores,⁴ G. Grenier,¹⁹ Ph. Gris,¹² J.-F. Grivaz,¹⁵ A. Grohsjean,¹⁷ S. Gründendahl,⁴⁷ M.W. Grünewald,²⁹ T. Guillemin,¹⁵ G. Gutierrez,⁴⁷ P. Gutierrez,⁷² A. Haas^d,⁶⁷ S. Hagopian,⁴⁶ J. Haley,⁵⁹ L. Han,⁶ K. Harder,⁴³ A. Harel,⁶⁸ J.M. Hauptman,⁵⁴ J. Hays,⁴² T. Head,⁴³ T. Hebbeker,²⁰ D. Hedin,⁴⁹ H. Hegab,⁷³ A.P. Heinson,⁴⁵ U. Heintz,⁷⁴ C. Hensel,²² I. Heredia-De La Cruz,³¹ K. Herner,⁶⁰ G. Hesketh^e,⁴³ M.D. Hildreth,⁵³ R. Hirosky,⁷⁸ T. Hoang,⁴⁶ J.D. Hobbs,⁶⁹ B. Hoeneisen,¹¹ M. Hohlfeld,²³ Z. Hubacek,^{9,17} V. Hynek,⁹ I. Iashvili,⁶⁶ Y. Ilchenko,⁷⁶ R. Illingworth,⁴⁷ A.S. Ito,⁴⁷ S. Jabeen,⁷⁴ M. Jaffré,¹⁵ D. Jamin,¹⁴ A. Jayasinghe,⁷² R. Jesik,⁴² K. Johns,⁴⁴ M. Johnson,⁴⁷ A. Jonckheere,⁴⁷ P. Jonsson,⁴² J. Joshi,²⁶ A.W. Jung,⁴⁷ A. Juste,³⁹ K. Kaadze,⁵⁶ E. Kajfasz,¹⁴ D. Karmanov,³⁶ P.A. Kasper,⁴⁷ I. Katsanos,⁶³ R. Kehoe,⁷⁶ S. Kermiche,¹⁴ N. Khalatyan,⁴⁷ A. Khanov,⁷³ A. Kharchilava,⁶⁶ Y.N. Kharzheev,³⁴ J.M. Kohli,²⁶ A.V. Kozelov,³⁷ J. Kraus,⁶¹ S. Kulikov,³⁷ A. Kumar,⁶⁶ A. Kupco,¹⁰ T. Kurča,¹⁹ V.A. Kuzmin,³⁶ J. Kvita,⁸ S. Lammers,⁵¹ G. Landsberg,⁷⁴ P. Lebrun,¹⁹ H.S. Lee,³⁰ S.W. Lee,⁵⁴ W.M. Lee,⁴⁷ J. Lellouch,¹⁶ L. Li,⁴⁵ Q.Z. Li,⁴⁷ S.M. Lietti,⁵ J.K. Lim,³⁰ D. Lincoln,⁴⁷ J. Linnemann,⁶¹ V.V. Lipaev,³⁷ R. Lipton,⁴⁷ Y. Liu,⁶ A. Lobodenko,³⁸ M. Lokajicek,¹⁰ R. Lopes de Sa,⁶⁹ H.J. Lubatti,⁷⁹ R. Luna-Garcia^f,³¹ A.L. Lyon,⁴⁷ A.K.A. Maciel,² D. Mackin,⁷⁷ R. Madar,¹⁷ R. Magaña-Villalba,³¹ S. Malik,⁶³ V.L. Malyshev,³⁴ Y. Maravin,⁵⁶ J. Martínez-Ortega,³¹ R. McCarthy,⁶⁹ C.L. McGivern,⁵⁵ M.M. Meijer,³³ A. Melnitchouk,⁶² D. Menezes,⁴⁹ P.G. Mercadante,⁴ M. Merkin,³⁶ A. Meyer,²⁰ J. Meyer,²² F. Miconi,¹⁸ N.K. Mondal,²⁸ G.S. Muanza,¹⁴ M. Mulhearn,⁷⁸ E. Nagy,¹⁴ M. Naimuddin,²⁷ M. Narain,⁷⁴ R. Nayyar,²⁷ H.A. Neal,⁶⁰ J.P. Negret,⁷ P. Neustroev,³⁸ S.F. Novaes,⁵ T. Nunnemann,²⁴ G. Obrant[‡],³⁸ J. Orduna,⁷⁷ N. Osman,¹⁴ J. Osta,⁵³ G.J. Otero y Garzón,¹ M. Padilla,⁴⁵ A. Pal,⁷⁵ N. Parashar,⁵² V. Parihar,⁷⁴ S.K. Park,³⁰ R. Partridge^d,⁷⁴ N. Parua,⁵¹ A. Patwa,⁷⁰ B. Penning,⁴⁷ M. Perfilov,³⁶ Y. Peters,⁴³ K. Petridis,⁴³ G. Petrillo,⁶⁸ P. Pétrouff,¹⁵ R. Piegai,¹ M.-A. Pleier,⁷⁰ P.L.M. Podesta-Lerma^g,³¹ V.M. Podstavkov,⁴⁷ P. Polozov,³⁵ A.V. Popov,³⁷ M. Prewitt,⁷⁷ D. Price,⁵¹ N. Prokopenko,³⁷ J. Qian,⁶⁰ A. Quadt,²² B. Quinn,⁶² M.S. Rangel,² K. Ranjan,²⁷ P.N. Ratoff,⁴¹ I. Razumov,³⁷ P. Renkel,⁷⁶ M. Rijssenbeek,⁶⁹ I. Ripp-Baudot,¹⁸ F. Rizatdinova,⁷³ M. Rominsky,⁴⁷ A. Ross,⁴¹ C. Royon,¹⁷ P. Rubinov,⁴⁷ R. Ruchti,⁵³ G. Safronov,³⁵ G. Sajot,¹³ P. Salcido,⁴⁹ A. Sánchez-Hernández,³¹ M.P. Sanders,²⁴ B. Sanghi,⁴⁷ A.S. Santos,⁵ G. Savage,⁴⁷ L. Sawyer,⁵⁷ T. Scanlon,⁴² R.D. Schamberger,⁶⁹ Y. Scheglov,³⁸ H. Schellman,⁵⁰ T. Schliephake,²⁵ S. Schlobohm,⁷⁹ C. Schwanenberger,⁴³ R. Schwienhorst,⁶¹ J. Sekaric,⁵⁵ H. Severini,⁷² E. Shabalina,²² V. Shary,¹⁷ A.A. Shchukin,³⁷ R.K. Shivpuri,²⁷ V. Simak,⁹ V. Sirotenko,⁴⁷ P. Skubic,⁷² P. Slattery,⁶⁸ D. Smirnov,⁵³ K.J. Smith,⁶⁶ G.R. Snow,⁶³ J. Snow,⁷¹ S. Snyder,⁷⁰

S. Söldner-Rembold,⁴³ L. Sonnenschein,²⁰ K. Soustruznik,⁸ J. Stark,¹³ V. Stolin,³⁵ D.A. Stoyanova,³⁷ M. Strauss,⁷² D. Strom,⁴⁸ L. Stutte,⁴⁷ L. Suter,⁴³ P. Svoisky,⁷² M. Takahashi,⁴³ A. Tanasijczuk,¹ M. Titov,¹⁷ V.V. Tokmenin,³⁴ Y.-T. Tsai,⁶⁸ K. Tschann-Grimm,⁶⁹ D. Tsybychev,⁶⁹ B. Tuchming,¹⁷ C. Tully,⁶⁵ L. Uvarov,³⁸ S. Uvarov,³⁸ S. Uzunyan,⁴⁹ R. Van Kooten,⁵¹ W.M. van Leeuwen,³² N. Varelas,⁴⁸ E.W. Varnes,⁴⁴ I.A. Vasilyev,³⁷ P. Verdier,¹⁹ L.S. Vertogradov,³⁴ M. Verzocchi,⁴⁷ M. Vesterinen,⁴³ D. Vilanova,¹⁷ P. Vokac,⁹ H.D. Wahl,⁴⁶ M.H.L.S. Wang,⁴⁷ J. Warchol,⁵³ G. Watts,⁷⁹ M. Wayne,⁵³ M. Weber,^{h, 47} L. Welty-Rieger,⁵⁰ A. White,⁷⁵ D. Wicke,²⁵ M.R.J. Williams,⁴¹ G.W. Wilson,⁵⁵ M. Wobisch,⁵⁷ D.R. Wood,⁵⁹ T.R. Wyatt,⁴³ Y. Xie,⁴⁷ R. Yamada,⁴⁷ W.-C. Yang,⁴³ T. Yasuda,⁴⁷ Y.A. Yatsunenko,³⁴ Z. Ye,⁴⁷ H. Yin,⁴⁷ K. Yip,⁷⁰ S.W. Youn,⁴⁷ J. Yu,⁷⁵ T. Zhao,⁷⁹ B. Zhou,⁶⁰ J. Zhu,⁶⁰ M. Zielinski,⁶⁸ D. Zieminska,⁵¹ and L. Zivkovic⁷⁴

(The D0 Collaboration*)

¹Universidad de Buenos Aires, Buenos Aires, Argentina

²LAFEX, Centro Brasileiro de Pesquisas Físicas, Rio de Janeiro, Brazil

³Universidade do Estado do Rio de Janeiro, Rio de Janeiro, Brazil

⁴Universidade Federal do ABC, Santo André, Brazil

⁵Instituto de Física Teórica, Universidade Estadual Paulista, São Paulo, Brazil

⁶University of Science and Technology of China, Hefei, People's Republic of China

⁷Universidad de los Andes, Bogotá, Colombia

⁸Charles University, Faculty of Mathematics and Physics,

Center for Particle Physics, Prague, Czech Republic

⁹Czech Technical University in Prague, Prague, Czech Republic

¹⁰Center for Particle Physics, Institute of Physics,

Academy of Sciences of the Czech Republic, Prague, Czech Republic

¹¹Universidad San Francisco de Quito, Quito, Ecuador

¹²LPC, Université Blaise Pascal, CNRS/IN2P3, Clermont, France

¹³LPSC, Université Joseph Fourier Grenoble 1, CNRS/IN2P3,

Institut National Polytechnique de Grenoble, Grenoble, France

¹⁴CPPM, Aix-Marseille Université, CNRS/IN2P3, Marseille, France

¹⁵LAL, Université Paris-Sud, CNRS/IN2P3, Orsay, France

¹⁶LPNHE, Universités Paris VI and VII, CNRS/IN2P3, Paris, France

¹⁷CEA, Irfu, SPP, Saclay, France

¹⁸IPHC, Université de Strasbourg, CNRS/IN2P3, Strasbourg, France

¹⁹IPNL, Université Lyon 1, CNRS/IN2P3, Villeurbanne, France and Université de Lyon, Lyon, France

²⁰III. Physikalisches Institut A, RWTH Aachen University, Aachen, Germany

²¹Physikalisches Institut, Universität Freiburg, Freiburg, Germany

²²II. Physikalisches Institut, Georg-August-Universität Göttingen, Göttingen, Germany

²³Institut für Physik, Universität Mainz, Mainz, Germany

²⁴Ludwig-Maximilians-Universität München, München, Germany

²⁵Fachbereich Physik, Bergische Universität Wuppertal, Wuppertal, Germany

²⁶Panjab University, Chandigarh, India

²⁷Delhi University, Delhi, India

²⁸Tata Institute of Fundamental Research, Mumbai, India

²⁹University College Dublin, Dublin, Ireland

³⁰Korea Detector Laboratory, Korea University, Seoul, Korea

³¹CINVESTAV, Mexico City, Mexico

³²Nikhef, Science Park, Amsterdam, the Netherlands

³³Radboud University Nijmegen, Nijmegen, the Netherlands and Nikhef, Science Park, Amsterdam, the Netherlands

³⁴Joint Institute for Nuclear Research, Dubna, Russia

³⁵Institute for Theoretical and Experimental Physics, Moscow, Russia

³⁶Moscow State University, Moscow, Russia

³⁷Institute for High Energy Physics, Protvino, Russia

³⁸Petersburg Nuclear Physics Institute, St. Petersburg, Russia

³⁹Institució Catalana de Recerca i Estudis Avançats (ICREA) and Institut de Física d'Altes Energies (IFAE), Barcelona, Spain

⁴⁰Stockholm University, Stockholm and Uppsala University, Uppsala, Sweden

⁴¹Lancaster University, Lancaster LA1 4YB, United Kingdom

⁴²Imperial College London, London SW7 2AZ, United Kingdom

⁴³The University of Manchester, Manchester M13 9PL, United Kingdom

⁴⁴University of Arizona, Tucson, Arizona 85721, USA

⁴⁵University of California Riverside, Riverside, California 92521, USA

⁴⁶Florida State University, Tallahassee, Florida 32306, USA

⁴⁷Fermi National Accelerator Laboratory, Batavia, Illinois 60510, USA

⁴⁸University of Illinois at Chicago, Chicago, Illinois 60607, USA

- ⁴⁹Northern Illinois University, DeKalb, Illinois 60115, USA
⁵⁰Northwestern University, Evanston, Illinois 60208, USA
⁵¹Indiana University, Bloomington, Indiana 47405, USA
⁵²Purdue University Calumet, Hammond, Indiana 46323, USA
⁵³University of Notre Dame, Notre Dame, Indiana 46556, USA
⁵⁴Iowa State University, Ames, Iowa 50011, USA
⁵⁵University of Kansas, Lawrence, Kansas 66045, USA
⁵⁶Kansas State University, Manhattan, Kansas 66506, USA
⁵⁷Louisiana Tech University, Ruston, Louisiana 71272, USA
⁵⁸Boston University, Boston, Massachusetts 02215, USA
⁵⁹Northeastern University, Boston, Massachusetts 02115, USA
⁶⁰University of Michigan, Ann Arbor, Michigan 48109, USA
⁶¹Michigan State University, East Lansing, Michigan 48824, USA
⁶²University of Mississippi, University, Mississippi 38677, USA
⁶³University of Nebraska, Lincoln, Nebraska 68588, USA
⁶⁴Rutgers University, Piscataway, New Jersey 08855, USA
⁶⁵Princeton University, Princeton, New Jersey 08544, USA
⁶⁶State University of New York, Buffalo, New York 14260, USA
⁶⁷Columbia University, New York, New York 10027, USA
⁶⁸University of Rochester, Rochester, New York 14627, USA
⁶⁹State University of New York, Stony Brook, New York 11794, USA
⁷⁰Brookhaven National Laboratory, Upton, New York 11973, USA
⁷¹Langston University, Langston, Oklahoma 73050, USA
⁷²University of Oklahoma, Norman, Oklahoma 73019, USA
⁷³Oklahoma State University, Stillwater, Oklahoma 74078, USA
⁷⁴Brown University, Providence, Rhode Island 02912, USA
⁷⁵University of Texas, Arlington, Texas 76019, USA
⁷⁶Southern Methodist University, Dallas, Texas 75275, USA
⁷⁷Rice University, Houston, Texas 77005, USA
⁷⁸University of Virginia, Charlottesville, Virginia 22901, USA
⁷⁹University of Washington, Seattle, Washington 98195, USA
- (Dated: October 19, 2011)

We present new direct constraints on a general Wtb interaction using data corresponding to an integrated luminosity of 5.4 fb^{-1} collected by the D0 detector at the Tevatron $p\bar{p}$ collider. The standard model provides a purely left-handed vector coupling at the Wtb vertex, while the most general, lowest dimension Lagrangian allows right-handed vector and left- or right-handed tensor couplings as well. We obtain precise limits on these anomalous couplings by comparing the data to the expectations from different assumptions on the Wtb coupling.

PACS numbers: 14.65.Ha, 12.60.Cn

The top quark was discovered in 1995 at the Tevatron [1, 2] via the pair production mode involving strong interactions. In 2009, the electroweak production of the top quark was observed by the D0 and CDF collaborations [3, 4]. At the Tevatron, the dominant production modes for single top quark are the s -channel (“ tb ”) [5] and t -channel (“ tqb ”) [6, 7] processes illustrated in Figure 1. A third process, usually called “associated production” in which the top quark is produced together with a W boson, has a small cross section at the Teva-

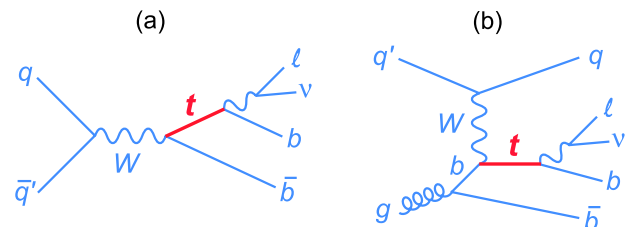


FIG. 1: Tree level Feynman diagrams for (a) tb and (b) tqb single top quark production.

*with visitors from ^aAugustana College, Sioux Falls, SD, USA, ^bThe University of Liverpool, Liverpool, UK, ^cUPIITA-IPN, Mexico City, Mexico, ^dSLAC, Menlo Park, CA, USA, ^eUniversity College London, London, UK, ^fCentro de Investigacion en Computacion - IPN, Mexico City, Mexico, ^gECFM, Universidad Autonoma de Sinaloa, Culiacán, Mexico, and ^hUniversität Bern, Bern, Switzerland. †Deceased.

tron compared to the tb and tqb processes [8]. Recently, we presented improved measurements of the single top quark production cross sections [9] and the observation of t -channel single top quark production [10].

The large mass of the top quark implies that it has large couplings to the electroweak symmetry breaking sector of the standard model (SM) and may have non-

standard interactions with the weak gauge bosons. Single top quark production provides a unique probe to study the interactions of the top quark with the W boson.

The most general, lowest dimension, CP -conserving Wtb vertex is given by [11]:

$$\begin{aligned} \mathcal{L} = & -\frac{g}{\sqrt{2}}\bar{b}\gamma^\mu(L_V P_L + R_V P_R)tW_\mu^- \\ & -\frac{g}{\sqrt{2}}\bar{b}\frac{i\sigma^{\mu\nu}q_\nu}{M_W}(L_T P_L + R_T P_R)tW_\mu^- + h.c., \end{aligned} \quad (1)$$

where M_W is the mass of the W boson, q_ν is the W boson four-momentum, $P_L = (1 - \gamma_5)/2$ is the left-handed projection operator, $P_R = (1 + \gamma_5)/2$ is the right-handed projection operator, $L_{V,T} = V_{tb} \cdot f_{L_{V,T}}$ and $R_{V,T} = V_{tb} \cdot f_{R_{V,T}}$. The form factor f_{L_V} (f_{L_T}) represents the left-handed vector (tensor) coupling, f_{R_V} (f_{R_T}) represents the right-handed vector (tensor) coupling, and V_{tb} is the Cabibbo-Kobayashi-Maskawa matrix element. In the SM, the Wtb coupling is left-handed with $L_V \equiv |V_{tb}| \simeq 1$ and $R_V = L_T = R_T = 0$. The magnitudes of the right-handed vector coupling and the tensor couplings can be indirectly constrained by the measured branching ratio of the $b \rightarrow s\gamma$ process [12]. Measurements of top quark decays in $t\bar{t}$ production, e.g. the W boson helicity [13, 14], can directly constrain the Lorentz structure of the Wtb vertex [15]. Assuming single top quarks are produced only via W boson exchange, the single top quark cross section is directly proportional to the square of the effective Wtb coupling. Moreover, the event kinematics and angular distributions are also sensitive to the existence of anomalous top quark couplings [16, 17]. Therefore, direct constraints on anomalous couplings can be obtained by measuring single top quark production [18].

This analysis uses the same data, event selection, and background modeling as the recent single top quark cross section measurements [9, 10]. We perform a study of anomalous Wtb couplings and obtain substantial improvements on the limits of these couplings following the general framework given in Ref. [18]. Out of the four couplings (L_V , L_T , R_V , R_T), we consider three cases pairing the left-handed vector coupling with each of the other three couplings: (L_V , R_V), (L_V , L_T) and (L_V , R_T), and for each case we assume the other two non-SM couplings are negligible. This pairing allows us to limit the complexity of the analysis, while increasing the statistical power and sensitivity for the anomalous coupling under study. We assume that single top quarks are produced exclusively through W boson exchange. Therefore other single top quark production mechanisms, such as flavor-changing neutral current interactions [19, 20], the decay of new scalar boson [21], or the exchange of new vector boson [22, 23] are not considered here. We also assume that the Wtb vertex dominates top quark production and decay, i.e., $|V_{td}|^2 + |V_{ts}|^2 \ll |V_{tb}|^2$. The results presented here supersede those contained in Ref. [18]. In addition

to the analysis of additional data and to the improvements in the event selection and background modeling used for the results presented in Ref. [9, 10], we use an updated calculation of the cross section as a function of the anomalous couplings which addresses a mistake present in the original analysis [18] (in that analysis the R_T and L_T couplings were accidentally swapped).

We select single top quark events which are expected to contain exactly one isolated large transverse momentum (p_T) electron or muon and large missing transverse energy (\cancel{E}_T). Events with 2, 3 or 4 jets are selected, and one or two of the jets are required to originate from the hadronization of long-lived b hadrons (b -jets) as determined by a multivariate b -tagging algorithm [24]. To increase the search sensitivity, we divide our data into six independent analysis channels, each with a different background composition and signal-to-background ratio. The channels are based on the number of identified b jets (1 or 2) and jet multiplicity (2, 3 or 4 jets). The signal selection efficiencies with different Wtb couplings, including branching fraction, trigger efficiencies and the b -tagging requirements, vary between 2.7% and 3.0% for tb and 1.9% and 2.2% for tqb production, estimated using Monte Carlo (MC) simulations. The ‘‘associated production’’ process gives a negligible contribution to this analysis.

Single top quark signal events with the SM and anomalous Wtb couplings are modeled using the COMPHEP-based MC event generator SINGLETOP [25] for a top quark mass $m_t = 172.5$ GeV using the CTEQ6M [26] parton distribution functions. The anomalous Wtb couplings are taken into account in both production and decay in the generated samples. The event kinematics for both s -channel and t -channel processes reproduce distributions from next-to-leading-order calculations [27, 28]. The decay of the top quark and the resulting W boson are carried out in the SINGLETOP [25] generator in order to preserve information about the spin of the particles. The theoretical cross sections for anomalous single top quark production ($s+t$ -channel) with $|V_{tb}| \simeq 1$ are 3.1 ± 0.3 pb if $f_{R_V} = 1$, 9.4 ± 1.4 pb if $f_{L_T} = 1$ or $f_{R_T} = 1$, and 10.6 ± 0.8 pb if $f_{R_T} = f_{L_V} = 1$ [16]. All other couplings are set to zero when calculating these cross sections. The SM single top quark production cross section is 3.3 ± 0.1 pb [8].

The main background contributions are those from W bosons produced in association with jets (W +jets), $t\bar{t}$ production, and multijet production in which a jet with high electromagnetic content mimics an electron, or a muon contained within a jet originating from the decay of a heavy-flavor quark (b or c quark) appears to be isolated. Diboson (WW , WZ , ZZ) and Z +jets processes add small additional contributions to the background. The $t\bar{t}$, W +jets, and Z +jets events are simulated with the ALPGEN leading-log MC generator [29]. The effect of anomalous Wtb couplings on kinematic distributions of

the $t\bar{t}$ background has been found to be negligible, thus only SM $t\bar{t}$ samples are considered in the analysis. Diboson processes are modeled using PYTHIA [30]. For all of the signal and background MC samples, PYTHIA is used to simulate parton showers and to model hadronization of all generated partons. The presence of additional $p\bar{p}$ interactions is modeled by events selected from random beam crossings matching the instantaneous luminosity profile in the data. All MC events are processed through a GEANT-based simulation [31] of the D0 detector and reconstructed using the same algorithm as data. Differences between simulation and data in lepton and jet reconstruction efficiencies and resolutions, jet energy scale, and b -tagging efficiencies are corrected in the simulation by applying correction functions measured from separate data samples. The $t\bar{t}$, Z +jets and diboson MC samples are scaled to their theoretical cross sections [32, 33]. We use data containing non-isolated leptons to model the multijet background. W +jets and multijet backgrounds are normalized by comparing the prediction for background to data before b -tagging. Details of the selection criteria and background modeling are given in Ref. [9].

The main contributions to the systematic uncertainty on the predicted number of events arise from the signal modeling, the jet energy scale (JES), jet energy resolution (JER), corrections to b -tagging efficiency and the correction for jet-flavor composition in W +jets events. These uncertainties affect the normalization of the distributions, and in some cases (JES, JER, and b -tagging) also change the differential distributions. There are smaller contributions due to limited statistics of the MC samples, uncertainties on the measured luminosity, and the trigger modeling. In addition, we also consider a signal cross section uncertainty (3.8% for tb and 5.3% for tqb) given by the NLO calculation. Details of systematic uncertainties are given in Ref. [9]. Table I lists the numbers of events expected and observed for each process as a function of jet multiplicity.

We use a multivariate analysis technique called Bayesian neural networks (BNN) [34] to separate the signal from the backgrounds. The BNN discriminant is trained using the lepton and jets four-vectors, a two-vector for \cancel{E}_T , and variables that include lepton charge and b -tagging information. In addition, four angular variables are added based on top quark spin and W boson helicity information to provide additional discriminating power. The total number of variables used in training for events with 2, 3, and 4 jets is 18, 22, and 26, respectively [9]. Three example distributions from some of the most sensitive variables are shown in Figure 2: the p_T spectrum of the lepton from the decay of the top quark and the cosine of the angles between the lepton, the leading b -tagged jet and the reconstructed top quark.

For each of the three scenarios, we consider the anomalous coupling sample as the signal when training BNN discriminants: for (L_V, R_V) , the signal is the single top

TABLE I: Numbers of expected and observed events in 5.4 fb^{-1} of integrated luminosity, with uncertainties including both statistical and systematic components. The single top quark contributions are normalized to their theoretical predictions.

| Source | 2 jets | 3 jets | 4 jets |
|-----------------------------------|-----------------|-----------------|-----------------|
| tb ($f_{L_T} = 1$) | 756 ± 42 | 344 ± 27 | 103 ± 15 |
| tqb ($f_{L_T} = 1$) | 103 ± 5.8 | 67 ± 6.3 | 28 ± 4.4 |
| tb ($f_{R_V} = 1$) | 105 ± 6.0 | 43 ± 3.8 | 12 ± 1.9 |
| tqb ($f_{R_V} = 1$) | 122 ± 7.2 | 61 ± 5.3 | 22 ± 3.7 |
| tb ($f_{R_T} = 1$) | 730 ± 38 | 316 ± 25 | 92 ± 14 |
| tqb ($f_{R_T} = 1$) | 117 ± 6.2 | 86 ± 8.6 | 40 ± 5.8 |
| tb ($f_{L_V} = f_{R_T} = 1$) | 607 ± 31 | 284 ± 21 | 86 ± 13 |
| tqb ($f_{L_V} = f_{R_T} = 1$) | 268 ± 15 | 167 ± 16 | 67 ± 10 |
| tb (SM, $f_{L_V} = 1$) | 104 ± 16 | 44 ± 7.8 | 13 ± 3.5 |
| tqb (SM, $f_{L_V} = 1$) | 140 ± 13 | 72 ± 9.4 | 26 ± 6.4 |
| $t\bar{t}$ | 433 ± 87 | 830 ± 133 | 860 ± 163 |
| W +jets | $3,560 \pm 354$ | $1,099 \pm 169$ | 284 ± 76 |
| Z +jets and dibosons | 400 ± 55 | 142 ± 41 | 35 ± 18 |
| Multijets | 277 ± 34 | 130 ± 17 | 43 ± 5.2 |
| Total SM prediction | $4,914 \pm 558$ | $2,317 \pm 377$ | $1,261 \pm 272$ |
| Data | 4,881 | 2,307 | 1,283 |

quark sample generated with $f_{R_V} = 1$; for (L_V, R_T) , the signal is the sample generated with $f_{R_T} = 1$; for (L_V, L_T) , the signal is the sample generated with $f_{L_T} = 1$. The background includes the SM single top quark sample with $f_{L_V} = 1$ and all the backgrounds described above. Each background component is represented in proportion to its expected fraction given by the background model. Figure 3 shows representative BNN discriminant output distributions for the three different scenarios with all six analysis channels combined.

We follow a Bayesian statistical approach [3, 35, 36] to compare data to the signal predictions given by different anomalous couplings using BNN discriminant output distributions. We compute a two-dimensional (2D) posterior probability as a function of $|V_{tb} \cdot f_{L_V}|^2$ and $|V_{tb} \cdot f_X|^2$, where $V_{tb} \cdot f_X$ is one of the two non-SM couplings $X = \{R_V, L_T\}$. For these two cases the single top quark contribution is represented by a superposition of two samples:

$$s = |V_{tb} \cdot f_{L_V}|^2 s_{L_V} + |V_{tb} \cdot f_X|^2 s_X, \quad (2)$$

where s_{L_V} (s_X) are the mean expected count of single top quarks for the assumptions $f_{L_V} = 1$ ($f_X = 1$) and the other couplings are set to zero. In the (L_V, R_T) scenario, the two couplings interfere, and to account for the effect of the interference, the single top quark contribution is represented by the superposition of three samples:

$$s = |V_{tb} \cdot f_{L_V}|^2 s_{L_V} + |V_{tb} \cdot f_{R_T}|^2 s_{R_T} + |V_{tb} \cdot f_{L_V}||V_{tb} \cdot f_{R_T}|(s_{L_V R_T} - s_{L_V} - s_{R_T}), \quad (3)$$

where s_{R_T} is the mean count assuming a left-handed tensor coupling only $f_{R_T} = 1$, and $s_{L_V R_T}$ is the one where

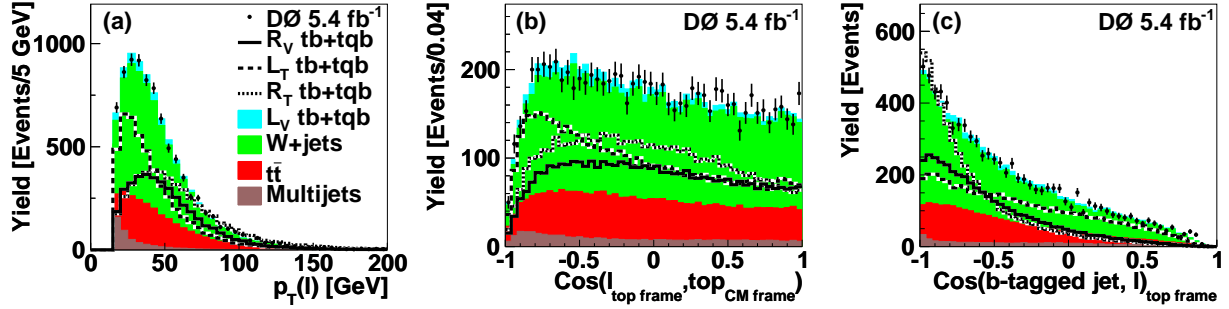


FIG. 2: Comparison of the SM backgrounds and data for selected discriminating variables with all channels combined: (a) lepton p_T , (b) cosine of the angle between the lepton (in the reconstructed top quark frame) and the reconstructed top quark (in the center of mass frame) and (c) cosine of the angle between the leading b -tagged jet and the lepton (both in the reconstructed top quark frame). Superimposed are the distributions from single top quark production (“ $tb + tqb$ ”) with one non-vanishing non-SM coupling (all other couplings set to zero) normalized to 10 times the SM single top quark cross section. The W +jets contributions include the smaller backgrounds from Z +jets and dibosons.

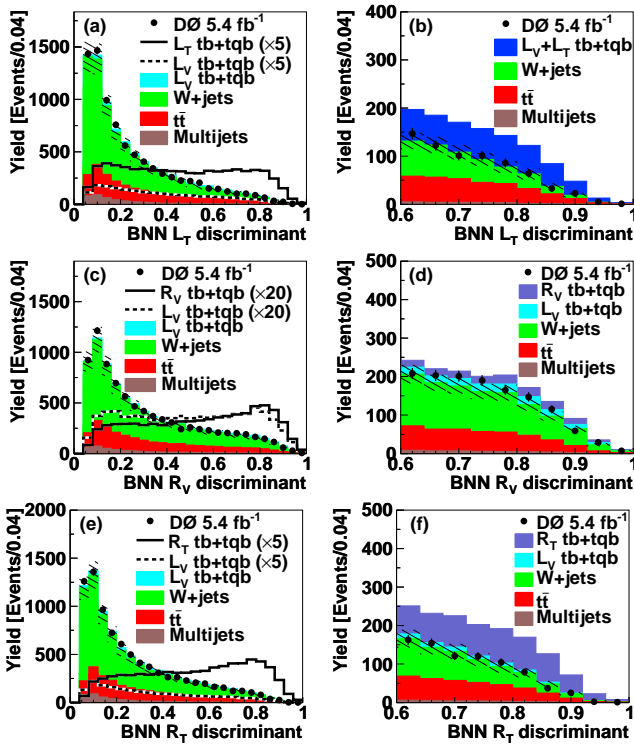


FIG. 3: The left column shows BNN discriminant output distributions of data and of the sum of the SM backgrounds with all channels combined for the whole discriminant range; superimposed are the distributions for the single top quark contributions scaled by (a) 5 times for the (L_V, L_T) scenario, (c) 20 times for the (L_V, R_V) scenario, and (e) 5 times for the (L_V, R_T) scenario. The right column shows BNN discriminant output distributions in the high discriminant region for (b) the (L_V, L_T) scenario, (d) the (L_V, R_V) scenario, and (f) the (L_V, R_T) scenario. The hatched bands give the uncertainty on the background sum. The W +jets contributions include the smaller backgrounds from Z +jets and dibosons.

both couplings $f_{L_V} = 1$ and $f_{R_T} = 1$. The last sample is indicated as “ $L_V + R_T$ ” in Fig. 3f. We assume a Poisson distribution for data counts and uniform prior

TABLE II: One-dimensional upper limits at 95% C.L. for anomalous Wtb couplings in the three scenarios.

| Scenario | Cross section | Coupling |
|--------------|---------------|-----------------------------------|
| (L_V, L_T) | < 0.60 pb | $ V_{tb} \cdot f_{L_T} ^2 < 0.06$ |
| (L_V, R_V) | < 2.81 pb | $ V_{tb} \cdot f_{R_V} ^2 < 0.93$ |
| (L_V, R_T) | < 1.21 pb | $ V_{tb} \cdot f_{R_T} ^2 < 0.13$ |

probability for nonnegative values of the SM and non-SM couplings. The output discriminants for the signal, backgrounds, and data are used to form a binned likelihood as a product over all six analysis channels and all bins, taking into account all systematic uncertainties and their correlations. The expected posterior probabilities are obtained by setting the number of data counts to be equal to the predicted sum of the signal and backgrounds.

Figure 4 shows the 2D posterior probability density distributions for the three scenarios. We do not observe significant deviations from the SM expectations and therefore compute 95% C.L. upper limits on the anomalous couplings by integrating out the left-handed vector coupling to get a one-dimensional posterior probability density. The measured values are given in Table II. With the SM constraint on the left-handed vector coupling, i.e. $|V_{tb} \cdot f_{L_V}| = 1$, the 95% C.L. limits on left-handed tensor, right-handed vector and tensor couplings are $|V_{tb} \cdot f_{L_T}|^2 < 0.05$, $|V_{tb} \cdot f_{R_V}|^2 < 0.50$ and $|V_{tb} \cdot f_{R_T}|^2 < 0.11$, respectively.

In summary, we have presented a search for anomalous Wtb couplings using 5.4 fb^{-1} of DØ data in the single top quark final state. We find no evidence for anomalous couplings and set 95% C.L. limits on these couplings. These represent improvements in the limits by factors of 2.6 to 5.0 in terms of couplings squared compared to the previous results [18] while a factor of approximately 2.5 is expected from the increase in integrated luminosity. This result represents the most stringent direct constraints on

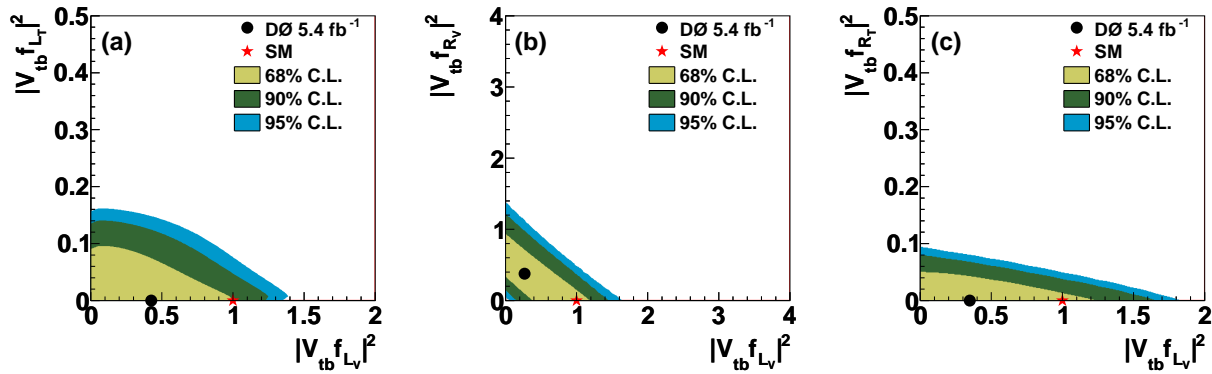


FIG. 4: Two-dimensional posterior probability density distributions for the anomalous couplings. The left row (a) shows the distribution for the (L_V, L_T) scenario, the middle row (b) for the (L_V, R_V) scenario, and the right row (c) for the (L_V, R_T) scenario. The dots represent the peak posterior from our data in comparison with the SM predictions.

anomalous Wtb interactions.

We thank the staffs at Fermilab and collaborating institutions, and acknowledge support from the DOE and NSF (USA); CEA and CNRS/IN2P3 (France); FASI, Rosatom and RFBR (Russia); CNPq, FAPERJ, FAPESP and FUNDUNESP (Brazil); DAE and DST (India); Colciencias (Colombia); CONACyT (Mexico); KRF and KOSEF (Korea); CONICET and UBACyT (Argentina); FOM (The Netherlands); STFC and the Royal Society (United Kingdom); MSMT and GACR (Czech Republic); CRC Program and NSERC (Canada); BMBF and DFG (Germany); SFI (Ireland); The Swedish Research Council (Sweden); and CAS and CNSF (China).

- [1] F. Abe *et al.* (CDF Collaboration), Phys. Rev. Lett. **74**, 2626 (1995).
- [2] S. Abachi *et al.* (D0 Collaboration), Phys. Rev. Lett. **74**, 2632 (1995).
- [3] V. M. Abazov *et al.* (D0 Collaboration), Phys. Rev. Lett. **103**, 092001 (2009).
- [4] T. Aaltonen *et al.* (CDF Collaboration), Phys. Rev. Lett. **103**, 092002 (2009).
- [5] S. Cortese and R. Petronzio, Phys. Lett. B **253**, 494 (1991).
- [6] S. S. D. Willenbrock and D. A. Dicus, Phys. Rev. D **34**, 155 (1986).
- [7] C.-P. Yuan, Phys. Rev. D **41**, 42 (1990).
- [8] N. Kidonakis, Phys. Rev. D **74**, 114012 (2006). The cross sections for the single top quark processes ($m_t = 172.5$ GeV) are 1.04 ± 0.04 pb (s -channel) and 2.26 ± 0.12 pb (t -channel).
- [9] V. M. Abazov *et al.* (D0 Collaboration), arXiv:1108.3091 [hep-ph], submitted to Phys. Rev. D.
- [10] V. M. Abazov *et al.* (D0 Collaboration), arXiv:1105.2788 [hep-ph], submitted to Phys. Lett. B.
- [11] G. L. Kane, G. A. Ladinsky, and C.-P. Yuan, Phys. Rev. D **45**, 124 (1992); J. A. Aguilar-Saavedra, Nucl. Phys. B **812**, 181 (2009).
- [12] F. Larios, M. A. Perez, and C.-P. Yuan, Phys. Lett. B **457**, 334 (1999); G. Burdman, M. C. Gonzalez-Garcia, and S. F. Novaes, Phys. Rev. D **61**, 114016 (2000); B. Grzadkowski and M. Misiak, Phys. Rev. D **78**, 077501 (2008); J. P. Lee and K. Y. Lee, Phys. Rev. D **78**, 056004 (2008), and references therein.
- [13] V. M. Abazov *et al.* (D0 Collaboration), Phys. Rev. Lett. **100**, 062004 (2008). V. M. Abazov *et al.* (D0 Collaboration), Phys. Rev. D **83**, 032009 (2011).
- [14] A. Abulencia *et al.* (CDF Collaboration) Phys. Rev. D **73**, 11103 (2006). A. Abulencia *et al.* (CDF Collaboration) Phys. Rev. D **75**, 052001 (2007). T. Aaltonen *et al.* (CDF Collaboration) Phys. Lett. B **674**, 160 (2009). T. Aaltonen *et al.* (CDF Collaboration) Phys. Rev. Lett. **105**, 042002 (2010).
- [15] V. M. Abazov *et al.* (D0 Collaboration), Phys. Rev. Lett. **102**, 092002 (2009).
- [16] E. Boos, L. Dudko, and T. Ohl, Eur. Phys. J. C **11**, 473 (1999).
- [17] D. O. Carlson, E. Malkawi, and C.-P. Yuan, Phys. Lett. B **337**, 145 (1994); E. Malkawi and C.-P. Yuan, Phys. Rev. D **50**, 4462 (1994); A. P. Heinson, A. S. Belyaev, and E. Boos, Phys. Rev. D **56**, 3114 (1997).
- [18] V. M. Abazov *et al.* (D0 Collaboration), Phys. Rev. Lett. **101**, 221801 (2008).
- [19] V. M. Abazov *et al.* (D0 Collaboration), Phys. Rev. Lett. **99**, 191802 (2007); V. M. Abazov *et al.* (D0 Collaboration), Phys. Lett. B **693**, 81 (2010).
- [20] T. Aaltonen *et al.* (CDF Collaboration) Phys. Rev. Lett. **102**, 151801 (2009).
- [21] V. M. Abazov *et al.* (D0 Collaboration), Phys. Rev. Lett. **102**, 191802 (2009).
- [22] V. M. Abazov *et al.* (D0 Collaboration), Phys. Lett. B **641**, 423 (2006); V. M. Abazov *et al.* (D0 Collaboration), Phys. Rev. Lett. **100**, 211803 (2008); V. M. Abazov *et al.* (D0 Collaboration), Phys. Lett. B **699**, 145 (2011).
- [23] T. Aaltonen *et al.* (CDF Collaboration) Phys. Rev. Lett. **103**, 041801 (2009).
- [24] V. M. Abazov *et al.* (D0 Collaboration), Nucl. Instrum. Methods in Phys. Res. A **620**, 490 (2010).
- [25] E. E. Boos *et al.*, Phys. Atom. Nucl. **69**, 1317 (2006). We use SINGLETOP version 4.2p1.
- [26] J. Pumplin *et al.*, J. High Energy Phys. **07**, 012 (2002). We use versions CTEQ6M for signal and CTEQ6L1 for background.
- [27] Z. Sullivan, Phys. Rev. D **70**, 114012 (2004).
- [28] J. M. Campbell, R. Frederix, F. Maltoni, and F. Tramonte

- tano, Phys. Rev. Lett. **102**, 182003 (2009).
- [29] M. L. Mangano *et al.*, J. High Energy Phys. **07**, 001 (2003). We use ALPGEN version 2.11.
- [30] T. Sjöstrand, S. Mrenna, and P. Skands, J. High Energy Phys. **08**, 026 (2006). We use version 6.409.
- [31] R. Brun and F. Carminati, CERN Program Library Long Writeup, Report No. W5013, 1993.
- [32] S. Moch and P. Uwer, Phys. Rev. D **78**, 034003 (2008). At $m_t = 172.5$ GeV, $\sigma(p\bar{p} \rightarrow t\bar{t} + X) = 7.46$ pb.
- [33] R. K. Ellis, Nucl. Phys. Proc. Suppl. **160**, 170 (2006). We use MCFM version 5.1.
- [34] R. M. Neal, *Bayesian Learning for Neural Networks* (Springer-Verlag, New York, 1996).
- [35] V. M. Abazov *et al.* (D0 Collaboration), Phys. Rev. Lett. **98**, 181802 (2007).
- [36] V. M. Abazov *et al.* (D0 Collaboration), Phys. Rev. D **78**, 012005 (2008).